Journal of the American College of Cardiology
© 2002 by the American College of Cardiology Foundation
Published by Elsevier Science Inc.

Vol. 40, No. 4, 2002
ISSN 0735-1097/02/$22.00
PII S0735-1097(02)02038-7

Influence of Microbubble Surface Charge on Capillary Transit and Myocardial Contrast Enhancement

Nicholas G. Fisher, MBBS, Jonathan P. Christiansen, MB, ChB, Alexander Klibanov, PhD, Ronald P. Taylor, PhD, Sanjiv Kaul, MD, FACC, Jonathan R. Lindner, MD, FACC
Charlottesville, Virginia

OBJECTIVE The goal of the study was to determine whether microbubble charge influences the microvascular retention of microbubble contrast agents.

BACKGROUND Interactions between serum proteins and lipid membranes are greater with anionic compared with neutral membranes. These interactions may influence the microvascular behavior of anionic lipid microbubbles.

METHODS Intravital microscopy of the cremaster muscle was performed in six wild-type mice and three C3-deficient mice during intravenous injection of lipid-shelled microbubbles with either a neutral or a negative charge. Both agents were prepared with and without a protective surface layer of polyethyleneglycol (PEG). Complement attachment to microbubbles was assessed by flow cytometry with flourescein isothiocyanate-conjugated anti-C3b monoclonal antibody. Myocardial contrast echocardiography was performed in six dogs to assess pulmonary and myocardial retention of microbubbles.

RESULTS Size-independent capillary retention of microbubbles, occurring for a few seconds to >10 min, was frequently observed with anionic, but rarely with neutral, microbubbles (4.3 ± 0.3 vs. 0.4 ± 0.1 mm^{-3}, $p < 0.01$). Anionic microbubble retention was reduced by 70% by surface PEG and was also markedly reduced in C3-deficient mice (1.4 ± 0.1 mm^{-3}, $p < 0.05$ vs. wild-type). Flow cytometry demonstrated complement attachment to only anionic microbubbles. Contrast echocardiography indicated both pulmonary and myocardial retention of only anionic microbubbles, the latter evidenced by persistent opacification >10 min after bolus intravenous injection.

CONCLUSIONS Lipid microbubbles with a net negative charge can be retained within capillaries via complement-mediated attachment to endothelium. This property may be useful for the development of ultrasound contrast agents that can be imaged late after venous injection. (J Am Coll Cardiol 2002;40:811–9) © 2002 by the American College of Cardiology Foundation

Most of the current microbubble ultrasound contrast agents have an intravascular rheology similar to that of red blood cells (1–3). Certain microbubble agents can adhere to activated leukocytes in postcapillary venules via cell-surface integrins or opsonization with complement, resulting in persistent myocardial opacification in regions of tissue inflammation (4,5). More recently, newer microbubble preparations have been shown to produce persistent opacification in the absence of inflammation despite the small size of the microbubbles (6). Myocardial persistence of these microbubbles appears to be due to capillary, rather than venular, retention (6).

A unique feature of one of the microbubble contrast agents that is retained within the capillaries is the negative charge on their lipid shells. Certain anionic lipids in the membranes of liposomes have been shown to activate complement and to enhance surface attachment of complement fragments and other plasma proteins (7–9). In this study we hypothesized that lipid microbubbles with a net negative charge (MB_{neg}) are retained in normal tissue due to complement-mediated interaction with the capillary endothelium. Because the presence of polyethyleneglycol (PEG) on the surface of lipid membranes may inhibit protein attachment (10,11), we also assessed the influence of a surface PEG layer on the microvascular behavior of these microbubbles.

METHODS

Microbubble preparation. To assess the effect of charge and the presence of a surface PEG layer on the behavior of microbubble contrast agents, four different lipid microbubble preparations were formulated: those with a neutral (MB_{neut}) or a net negative (MB_{neg}) surface charge, each with or without a surface PEG layer (PEG^+ or PEG^-). For MB_{neut}, decafluorobutane gas was sonicated with an aqueous dispersion of 1.6 mg·ml^{-1} distearoyl phosphatidylcholine (Avanti Polar Lipids, Alabaster, Alabama) and PEG-5000, which was used to facilitate bubble formation. For MB_{neg}, 0.8 mg·ml^{-1} of dipalmitoyl phosphatidylglycerol (Avanti Polar Lipids) was added to the dispersion. For microbubbles with a protective surface PEG layer, 0.8 mg·ml^{-1} PEG-40 stearate (Sigma, St. Louis, Missouri) was added to the dispersion before sonication. For microscopy

From the Cardiovascular Imaging Center, Cardiovascular Division, University of Virginia, Charlottesville, Virginia. Supported by grants (R01-HL48890 and R01-HL65704) from the National Institutes of Health, Bethesda, Maryland. Dr. Christiansen is a recipient of a Postdoctoral Fellowship Award from the American Heart Association, Mid-Atlantic Affiliate, Baltimore, Maryland. Dr. Lindner is the recipient of a Mentored Clinical Scientist Development Award (K08-HL03810).

Manuscript received January 4, 2002; revised manuscript received April 4, 2002, accepted May 7, 2002.

Abbreviations and Acronyms

C3−/− = C3-deficient
FITC = fluorescein isothiocyanate
LV = left ventricular
mAb = monoclonal antibody
MB_{neg} = lipid microbubbles with a net negative charge
MB_{neut} = lipid microbubbles with a net neutral charge
PEG = polyetheleneglycol
PEG^- = without a surface polyetheleneglycol layer
PEG^+ = with a surface polyetheleneglycol layer
RV = right ventricular
VI = video intensity

studies, microbubbles were fluorescently labeled with 0.025 $mg \cdot ml^{-1}$ dioctadecyl-oxacarbocyanine (DiO, Molecular Probes, Eugene, Oregon). All microbubbles were washed, and their concentration and size distribution were determined by electrozone sensing with a Coulter Multisizer IIe (Beckman-Coulter, Fullerton, California).

Microbubble charge was determined by their zeta potential measured by laser Doppler velocimetry (Zetaplus, Brookhaven Instruments, Holtsville, New York) (12) of approximately 1×10^7 microbubbles dispersed in 1 mM KCl. Results of two separate measurements were averaged.

Complement attachment to microbubbles. Flow cytometry of microbubbles was performed to determine whether charge and the presence of PEG influenced serum complement attachment to the microbubble surface. For each preparation 1×10^7 microbubbles were combined with 500 μl of human serum for 5 min at 37°C and washed twice. Aliquots of 2×10^6 serum-exposed or control microbubbles were combined with a fluorescein isothiocyanate (FITC)-labeled murine antihuman C3b monoclonal antibody (mAb) (3E7) or an FITC-labeled IgG_1 isotype-control antibody for 10 min. Microbubbles were washed and analyzed on a FACSCalibur (Becton Dickinson, Franklin Lakes, New Jersey) to generate histograms of green fluorescent intensity.

Intravital microscopy. The study was approved by the Animal Research Committee at the University of Virginia. Intravital microscopy was performed to assess the microvascular behavior of the four microbubble preparations in the normal circulation of nine male wild-type C57BL/6 mice and three male C3-deficient (C3−/−) mice (B6.1229S4-C3, Jackson Laboratory, Bar Harbor, Maine). The mice were anesthetized with an intraperitoneal injection of a solution containing ketamine hydrochloride, xylazine and atropine. A cremaster muscle was exteriorized, prepared for intravital microscopy, and superfused continuously with isothermic bicarbonate-buffered saline. Observations were made with an Axioskop2-FS microscope (Carl Zeiss, Inc., Thornwood, New York) with a saline-immersion objective (×20/0.5 N.A.) under combined transillumination and fluorescent epi-illumination (469–500 nm excitation filter). Video recordings were made with a high-resolution CCD camera (C2400, Hamamatsu Photonics, Hamamatsu, Japan) that was interfaced with a video time display unit (VTG-33 for A Ltd., Tokyo, Japan) and connected to an S-VHS recorder (S9500, JVC, Elmwood Park, New Jersey).

For each microbubble type, 3×10^7 of DiO-labeled microbubbles were injected via the jugular vein in random order separated by 20-min intervals. Twenty optical fields (total tissue volume 4.2 ± 10^{-3} cm^3) were observed 2 min, 6 min, and 12 min after each injection. Static microbubbles were defined as those that were stationary for >3 s. After each injection, randomly selected arterioles were recorded, and velocity was measured with a dual-slit photodiode (CircuSoft Instrumentation, Hockessin, Delaware) for calculation of arteriolar blood flow and shear rate. The diameter of retained microbubbles was measured off-line using video calipers.

Contrast echocardiography. Contrast echocardiography was performed to estimate the relative entrapment of microbubbles in the pulmonary as well as the myocardial microcirculation after intravenous bolus injection of the different microbubble agents. Six anesthetized, open-chest dogs were used for this purpose. Power-pulse inversion imaging was performed with an HDI-5000 system (Philips Ultrasound, Bothell, Washington) in the basal short-axis plane using a saline bath as an acoustic interface. A mechanical index of 0.1 and a pulse-repetition frequency of 2,500 Hz were used. Gain settings were optimized at the beginning of each experiment and held constant. Images were saved on magneto-optical disk and analyzed off-line (HDI Lab, Philips Ultrasound).

To determine their pulmonary retention, 2×10^6 microbubbles (either $MB_{neut}PEG^+$ or $MB_{neg}PEG^-$) were injected as an intravenous bolus during acquisition of end-diastolic frames at every one cardiac cycle. Video intensity (VI) in the right ventricular (RV) and left ventricular (LV) cavities was measured, and time-intensity data were fit to a γ-variate function: $y = Ate^{-\alpha t}$, where y is the VI at time t, A is a scaling factor and α reflects the mean transit rate (13). The integral for each time-intensity curve was calculated by A/α^2 to represent the total number of microbubbles transiting through each cavity (14). A pulmonary retention index was calculated by the ratio of the LV to RV integrals. End-diastolic and end-systolic RV short-axis dimensions were measured by video calipers immediately before and 1 min after injection.

To assess their myocardial retention, 1×10^9 microbubbles were injected as an intravenous bolus, and end-systolic frames were acquired. In order to minimize microbubble destruction, imaging was performed every one cardiac cycle for 1 min and every 20 cardiac cycles thereafter. Ten minutes after injection, VI was measured from the anterior myocardium. The absence of signal from freely circulating microbubbles was verified by the absence of myocardial opacification from microbubble replenishment after a brief sequence of high-power (mechanical index 1.1) pulses.

Table 1. Size and Charge Characteristics for Microbubbles

	$MB_{neut}PEG^-$	$MB_{neut}PEG^+$	$MB_{neg}PEG^-$	$MB_{neg}PEG^+$
Mean diameter (μm)*	2.3 ± 0.3	2.8 ± 0.5	2.6 ± 0.3	2.7 ± 0.4
Zeta potential (mV)	−3	−1	−73	−69

*Analysis of variance, p = NS.
MB_{neg} = lipid microbubbles with a net negative charge; MB_{neut} = lipid microbubbles with a net neural charge; PEG = polyetheleneglycol.

Microbubble acoustic signal. In vitro experiments were performed to determine whether the presence of PEG influenced the acoustic signal from microbubbles. Either $MB_{neut}PEG^+$ or $MB_{neut}PEG^-$ (5×10^7) was added to a 500-ml saline bath containing a magnetic stir bar. Measurements of acoustic intensity were made using identical settings used in the clinical experiments from a 2 cm^2 region-of-interest at a depth of 5 to 7 cm. Measurements were made 30 s after addition of microbubbles. Three separate measurements were averaged for each agent.

Statistical methods. Data are expressed as the mean ± SD. Comparisons of continuous variables were made using the Student *t* test (paired) and repeated-measures analysis of variance. Categorical values of microbubble diameter were compared by chi-square. Differences were considered significant at $p < 0.05$.

RESULTS

Microbubble size, charge, and microvascular behavior. The mean microbubble size before injection was similar for the four different microbubble preparations (Table 1). The zeta potential, reflecting microbubble surface charge, was highly negative for MB_{neg} and was not substantially altered by a surface PEG layer (Table 1). Microvascular flow and shear rates in the cremasteric vessels were similar after injection of the different microbubble preparations. In wild-type mice, retention of MB_{neut} in the cremaster was uncommon, regardless of the presence or absence of PEG (Fig. 1). In comparison, MB_{neg} retention was much more frequent, although it was substantially reduced (by ≈70%) by the presence of PEG. In C3−/− mice, MB_{neg} retention was markedly reduced compared with wild-type mice, regardless of the presence or absence of PEG, and was similar in extent to that for MB_{neut} (Fig. 1). Microbubbles were retained exclusively in capillaries or very small arterioles (<10 μm).

The sizes of $MB_{neg}PEG^-$ and $MB_{neut}PEG^+$ were similar before injection (Fig. 2A). Microbubbles that were retained within the cremasteric microcirculation tended to be large, although the diameters for retained $MB_{neg}PEG^-$ were smaller than $MB_{neut}PEG^+$ (Fig. 2B). The infrequent retention of $MB_{neut}PEG^+$ invariably resulted in cessation of capillary flow. Retention of $MB_{neg}PEG^-$ was occasionally associated with residual flux of RBCs around static microbubbles, suggesting that microbubble size was not the sole mechanism for $MB_{neg}PEG^-$ retention.

The duration of capillary retention varied from several seconds to >10 min for individual microbubbles. Capillary retention tended to decrease over time, although this was significant only for $MB_{neg}PEG^-$ (4.3 ± 0.3, 2.9 ± 0.5, and

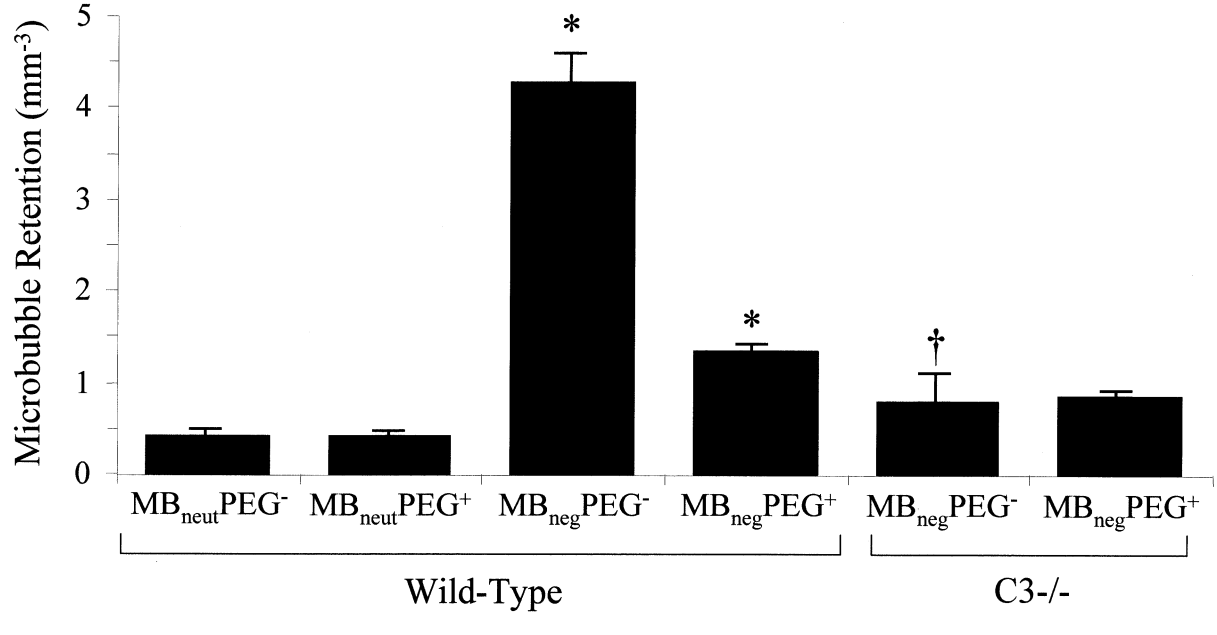

Figure 1. Mean (± SEM) number of microbubbles retained within the cremasteric microcirculation of wild-type and C3-deficient (C3−/−) mice after injection of 3×10^7 microbubbles. *$p < 0.01$ all other microbubbles in wild-type mice; †$p < 0.01$ vs. MB_{neg} in wild-type mice. MB_{neg} = lipid microbubbles with a net negative charge; MB_{neut} = lipid microbubbles with a net neutral charge; PEG = polyetheleneglycol.

JACC Vol. 40, No. 4, 2002
August 21, 2002:811–9

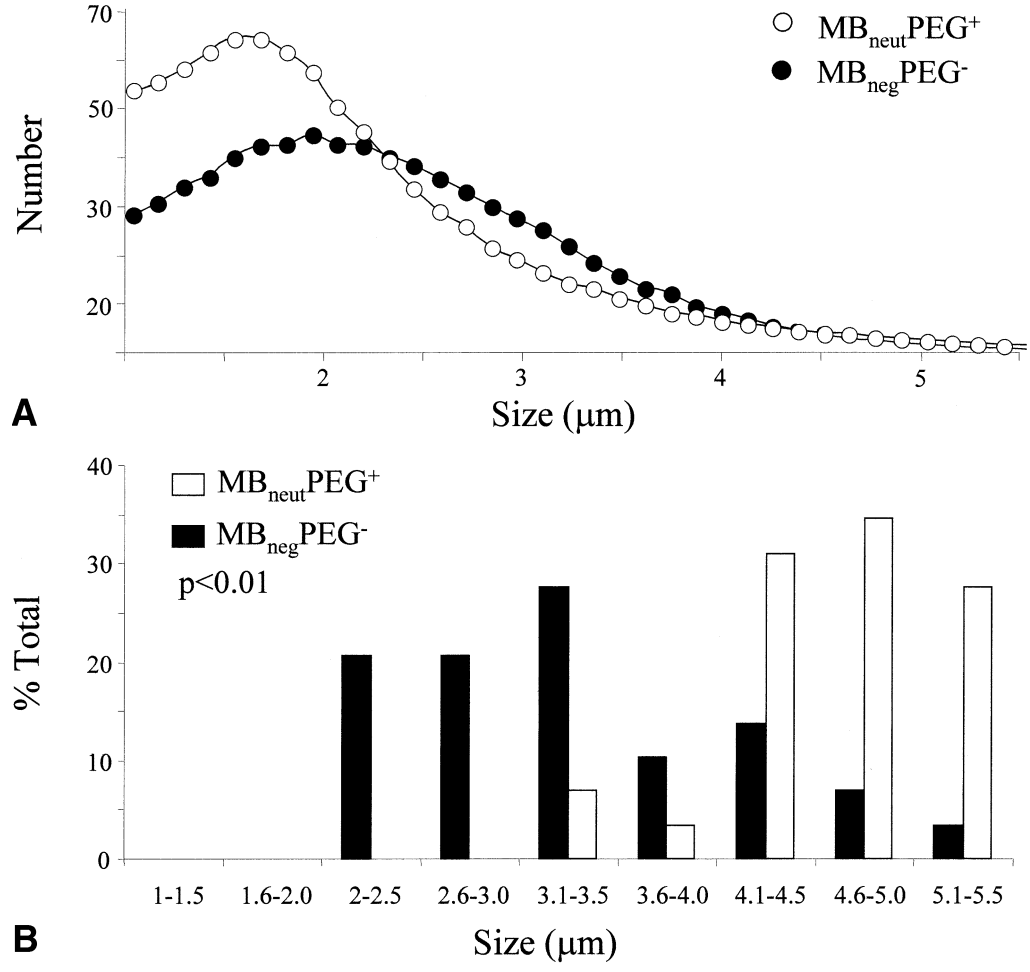

Figure 2. Size distribution of all microbubbles before injection **(A)** and those retained within the microcirculation **(B)**. MB_{neg} = lipid microbubbles with a net negative charge; MB_{neut} = lipid microbubbles with a neutral charge; PEG = polyetheleneglycol.

$2.1 \pm 0.9\ mm^{-3}$ at 2, 6, and 12 min, respectively, $p < 0.05$). The time-dependent decrease in retention was due mostly to gradual reduction in the frequency of brief static events.

Complement deposition on microbubble shell. Serum complement attachment to microbubble shells was assessed by flow cytometry. Figure 3 illustrates examples of flow cytometry data for $MB_{neut}PEG^{+}$ (Fig. 3A) and $MB_{neg}PEG^{-}$ (Fig. 3B) representing the two extremes with respect to capillary retention. Histograms of green fluorescent intensity are shown for microbubbles incubated with serum and FITC-conjugated control mAb (curve A), with FITC-conjugated anti-C3b mAb alone without serum (curve B), or with serum and FITC-conjugated anti-C3b mAb (curve C). Fluorescent intensity for $MB_{neut}PEG^{+}$ exposed to serum and FITC-conjugated anti-C3b mAb was very low and was similar to that found for control experiments. Fluorescent intensity for $MB_{neg}PEG^{-}$ exposed to serum and FITC-conjugated anti-C3b mAb was much greater than corresponding control experiments, indicating attachment of C3b to the surface of these microbubbles. Surface attachment of C3b, reflected by microbubble mean fluorescent intensity, was much greater for MB_{neg} compared with MB_{neut}, and was minimally inhibited by the presence of PEG on the surface (Fig. 4). The mean fluorescent intensity was low (<50 U) for all control experiments.

Pulmonary and myocardial retention of microbubbles. In vitro imaging experiments demonstrated similar VI for equal concentrations of $MB_{neut}PEG^{-}$ and $MB_{neut}PEG^{+}$ (37 ± 2 vs. 35 ± 3, $p = 0.51$). These data indicate that the surface layer of PEG produced minimal viscoelastic and acoustic damping. Examples of time-intensity curves from LV and RV cavities after a venous bolus injection of microbubbles are shown in Figure 5. The area under the curve for the LV relative to the RV was smaller for $MB_{neg}PEG^{-}$ (panel B) compared with $MB_{neut}PEG^{+}$ (panel A), indicating greater pulmonary retention for the latter. These differences were quantified by the LV:RV integral of the curves, which was significantly smaller for $MB_{neg}PEG^{-}$ compared with $MB_{neut}PEG^{+}$ (0.35 ± 0.16 vs. 0.66 ± 0.15, $p < 0.001$), indicating greater pulmonary retention for the former. These findings also imply that the differences in cremasteric retention in wild-type mice for neutral compared with anionic microbubbles (Fig. 1) may have been underestimated because fewer of the anionic microbubbles

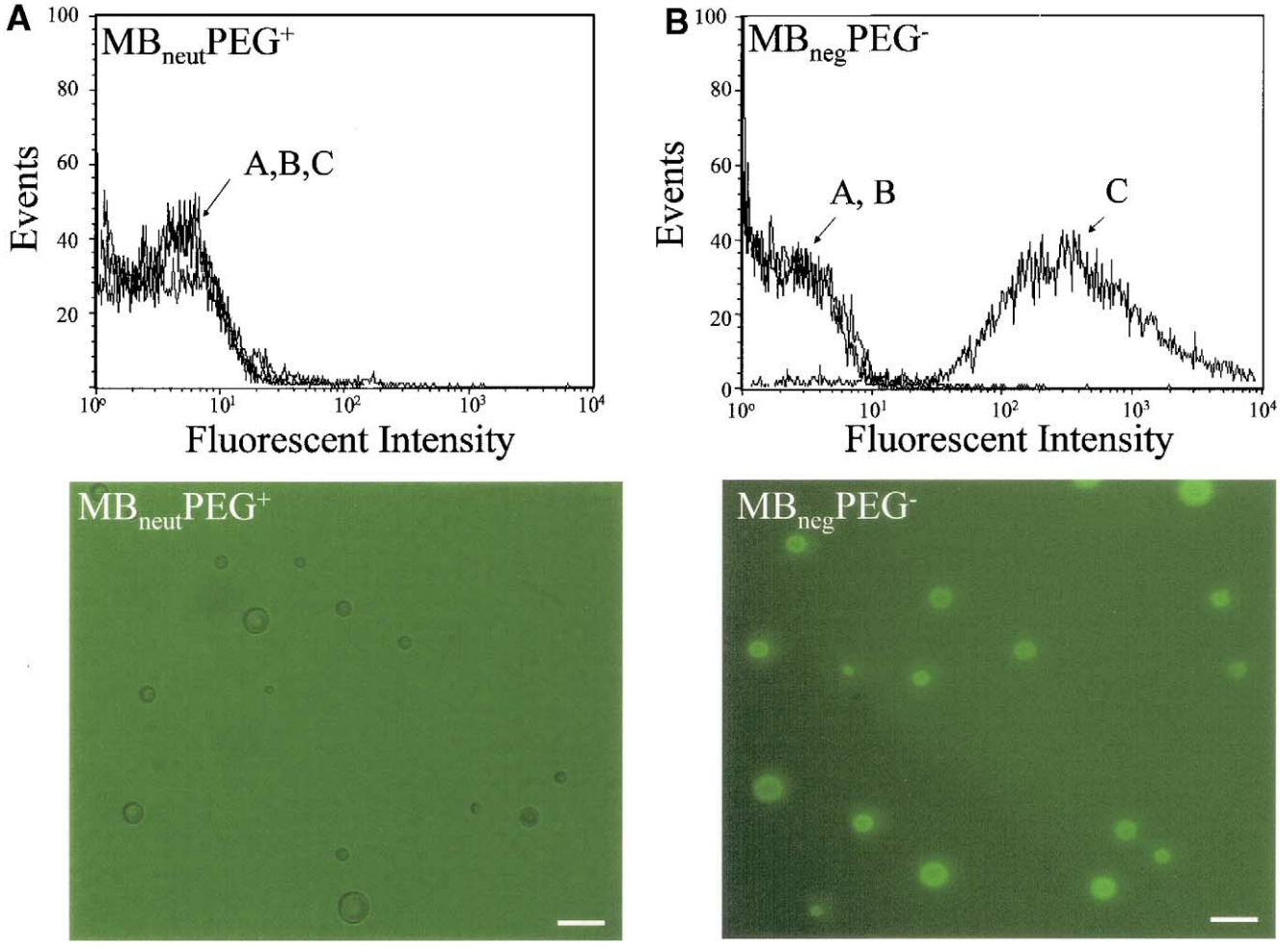

Figure 3. Examples of flow cytometry data for lipid microbubbles with a net neutral charge with polyetheleneglycol ($MB_{neut}PEG^+$) and lipid microbubbles with a net negative charge without polyetheleneglycol ($MB_{neg}PEG^-$). Histograms of **green fluorescent** intensity are shown for microbubbles incubated with serum and florescein isothiocyanate (FITC)-conjugated control monoclonal antibody (mAb) **(A)**, with FITC-conjugated anti-C3b mAb alone without serum **(B)**, or with serum and FITC-conjugated anti-C3b mAb **(C)**. Corresponding fluorescent microscopy images from *c* samples are shown at the **bottom** (scale bars = 5 μm).

would be expected to reach the systemic microcirculation. Microbubble injections did not produce any significant change in RV dimensions, even for $MB_{neg}PEG^-$ ($-5 \pm 5\%$ and $-5 \pm 9\%$ for changes in end-systolic and diastolic diameters, $p = 0.40$ and 0.61, respectively).

Figure 6 illustrates examples of myocardial time-intensity curves obtained 10 min after intravenous injection of $MB_{neut}PEG^+$ and $MB_{neg}PEG^-$ microbubbles, representing the two extremes for microbubble retention seen on intravital microscopy. Persistent myocardial opacification late after injection was seen only for $MB_{neg}PEG^-$. In all animals myocardial contrast enhancement was detected 10 min after injection of $MB_{neg}PEG^-$ (background-subtracted VI of 4 ± 2 U) but was not seen for $MB_{neut}PEG^+$ (background-subtracted VI of <1.0). As illustrated in Fig. 6, the presence of few residual circulating microbubbles was verified for each experiment by lack of reappearance of microbubble signal after a high-power pulse sequence that destroyed retained microbubbles.

DISCUSSION

This is the first study to demonstrate that a net negative shell charge can result in capillary retention of microbubbles within the normal microcirculation via a mechanism other than lodging, and that this effect can be substantially reduced by the presence of a surface layer of PEG. We have also demonstrated that retention is mediated by attachment of activated C3b to the microbubble surface. Because this property of microbubbles results in prolonged myocardial opacification after a venous injection, modulating shell surface charge may be an effective means of optimizing microbubble kinetics for perfusion and viability imaging.

It has long been recognized that liposomes possessing a net negative charge have a shorter intravascular lifespan compared with their neutral counterparts due to complement-mediated uptake by the reticuloendothelial system (8,9). Accordingly, lipid-shelled microbubble contrast agents have been composed mostly of lipids that

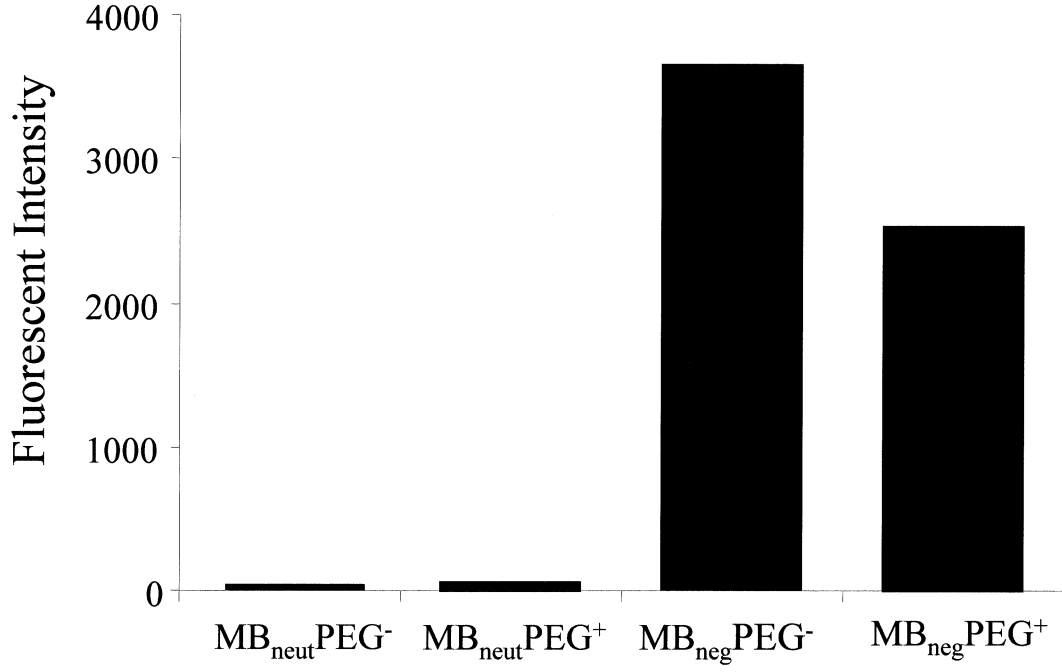

Figure 4. Degree of C3b attachment to microbubbles, determined by mean fluorescent intensity (*y*-axis) measured by flow cytometry of microbubbles incubated with serum and fluorescein isothiocyanate (FITC)-conjugated anti-C3b monoclonal antibody.

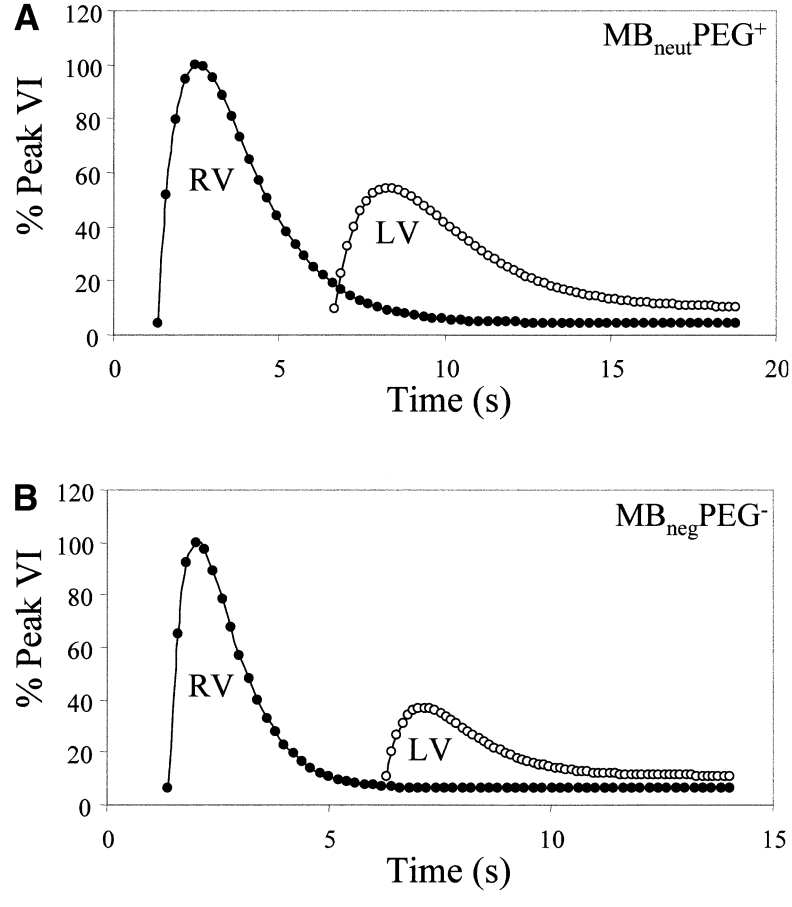

Figure 5. Examples of time versus VI curves for the right ventricular and left ventricular cavities after bolus intravenous injection of lipid microbubbles with a net neutral charge polyetheleneglycol ($MB_{neut}PEG^{+}$) **(A)** and lipid microbubbles with a net negative charge polyetheleneglycol ($MB_{neg}PEG^{-}$) **(B)**. See text for details. LV = left ventricular; RV = right ventricular.

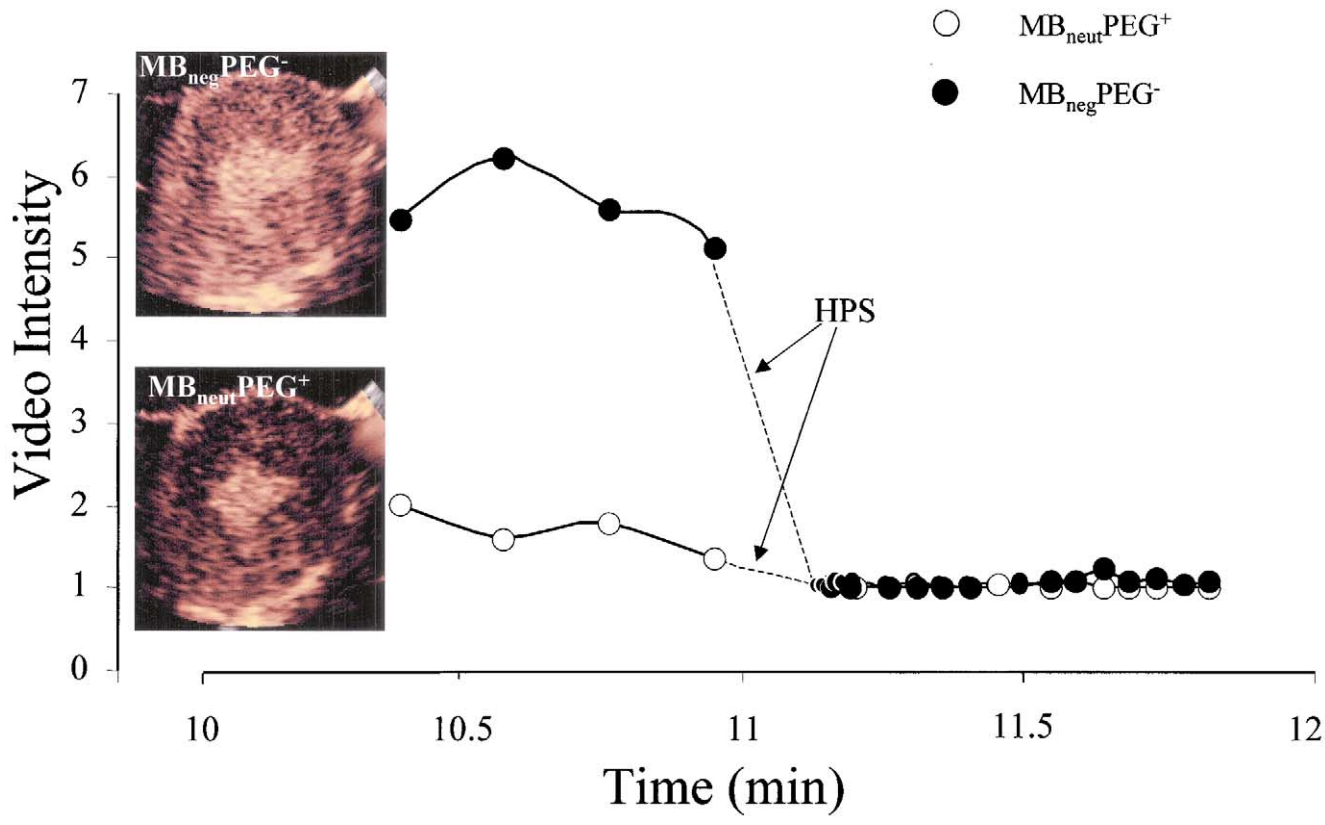

Figure 6. Representative myocardial contrast enhancement images and time versus VI data from the anterior myocardium of one dog acquired >10 min after intravenous injections of lipid microbubbles with a net negative charge without polyetheleneglycol ($MB_{neg}PEG^{-}$) **(solid circles)** and lipid microbubbles with a net neutral charge with polyetheleneglycol ($MB_{neut}PEG^{+}$) **(open circles)**. Data are shown before and after a brief high-power ultrasound sequence (HPS).

possess a neutral charge at physiologic pH in order to optimize their intravascular stability and prolong their circulation times. There has been no evidence for systemic microvascular retention of encapsulated microbubble contrast agents until just recently when it was determined that a small fraction of a negatively charged lipid microbubble preparation could be retained in the capillaries (6).

In the current study, we demonstrated late myocardial contrast enhancement after injection of anionic microbubbles at a time when freely circulating microbubbles had been cleared from the blood pool. Direct observations of the skeletal muscle microcirculation confirmed that late opacification was due to capillary retention from microbubble-endothelial interactions rather than size-dependent entrapment. By comparing the microbubble behavior in wild-type and C3−/− mice, we were able to determine that serum complement was responsible for the attachment of anionic microbubbles to the capillary endothelium. We have previously demonstrated that lipid microbubbles with a weak negative charge can be retained within inflamed tissue due to complement-mediated attachment to activated leukocytes within venules (4). We have further shown that increasing the negative charge by addition of phosphatidylserine on the surface markedly enhances this process (5). In the current study, lipid microbubbles with a much stronger negative charge were studied in the absence of inflammation. Leukocyte retention was very rarely seen due to the lack of leukocyte activation and adhesion in venules. Retention instead occurred primarily in capillaries. Although the precise mechanism responsible for endothelial attachment of these microbubbles is not known, it is likely that C3b binds to either membrane-associated complement proteins (CD46) or decay-accelerating factor (CD55). These proteins are expressed on the endothelial surface and are known to bind to C3b and convert it to the inactive C3bi (15,16). Reasons for preferential capillary retention of microbubbles include selective expression of C3b-binding proteins on the capillary endothelium, lower shear forces and size-related requirement for adequate surface area to support attachment.

Although retention of $MB_{neg}PEG^{-}$ was markedly reduced in C3−/− mice, some residual retention was observed, the extent of which was similar to MB_{neut} (with or without PEG) retention in wild-type mice. The microbubbles responsible for this "background" retention were relatively large (>4 μm) and were likely entrapped because of their size. These large microbubbles may have evaded pulmonary capillary filtering due to a small degree of pulmonary shunting that may allow few of the larger microbubbles to arrive in the systemic circulation (17). Alternatively, other serum proteins that attach to negatively

charged lipid surfaces, such as fibrinogen, fibronectin, and apolipoproteins, may have contributed to residual retention (18).

The presence of PEG on the surface of liposomes has been shown to inhibit electrostatic and hydrophobic interactions between serum proteins and lipid membranes (10,11). Reduced complement deposition on the surface of PEG-containing liposomes may be responsible for their longer circulating times by inhibiting uptake by reticulendothelial cells (19,20). Many of the lipid microbubbles in clinical use possess a protective PEG layer on the shell surface. In this study, incorporation of PEG into the lipid shell inhibited capillary retention of anionic microbubbles by approximately 70%. Yet flow cytometry revealed that C3b attachment to negatively charged microbubbles was only mildly inhibited by PEG. These results suggest that PEG reduced microbubble-endothelial interactions by steric hindrance (21). In other words, PEG did little to prevent complement deposition on the lipid shell but, instead, provided a barrier to complement binding to endothelial cell-surface receptors.

Microvascular retention of microbubbles with a strong negative charge raises questions regarding their safety. Dodecafluoropentane emulsion, an ultrasound contrast agent formerly used in the experimental setting, produced excellent myocardial opacification after clearance from the circulating blood pool (22). However, its safety was called into question due to marked pulmonary retention (22,23), which may have been aggravated by volume expansion of this nonencapsulated agent. Our data suggests that size-independent pulmonary retention of encapsulated microbubbles after venous injection is enhanced by a negative charge on the shell. The much lower signal for the LV compared with RV seen for all microbubbles does not necessarily indicate a large retention fraction in the lung. Large microbubbles contribute disproportionately to the total signal from microbubbles (24). Hence, pulmonary retention of the few large (>5 μm) microbubbles would be expected to result in a disproportionate large decrease in the LV cavity signal. Nevertheless, even modest pulmonary retention could interfere with pulmonary gas exchange, especially in patients with lung disease.

Our initial investigation of the in vivo kinetics of highly anionic microbubbles indicated that these agents could provide information on myocardial perfusion when imaged early after a bolus injection and on myocardial viability on delayed imaging (6). For this type of clinical application, it may be possible to modulate the net charge and PEG content of lipid microbubbles to an ideal level where myocardial opacification is optimal, yet systemic or pulmonary toxicity are minimal. Charge optimization may also be important because myocardial retention can be offset by less recirculation caused by complement-mediated reticuloendothelial uptake of highly charged microbubbles. In order to achieve these goals, it will be necessary to determine the exact mechanism whereby complement mediates the interaction between anionic microbubbles and capillary endothelium. It will also be important to determine whether the capillary retention of strongly anionic microbubbles is enhanced in settings where complement is activated systemically or locally. Nonetheless, our current results provide insight into how interactions between ultrasound contrast agents and serum proteins can affect their behavior in the normal microcirculation.

Reprint requests and correspondence: Dr. Jonathan R. Lindner, Cardiovascular Division, Box 800158, Medical Center, University of Virginia, Charlottesville, Virginia 22908-0158. E-mail: jlindner@virginia.edu.

REFERENCES

1. Keller MW, Segal SS, Kaul S, Duling B. The behaviour of sonicated albumin microbubbles in the microcirculation: a basis for their use during myocardial contrast echocardiography. Circ Res 1989;65:458–67.
2. Jayaweera AR, Edwards N, Glasheen WP, Villanueva FS, Abbott RD, Kaul S. In vivo myocardial kinetics of air filled albumin microbubbles during myocardial contrast echocardiography: comparison with radiolabeled red blood cells. Circ Res 1994;74:1157–65.
3. Lindner JR, Song J, Jayaweera AR, Sklenar J, Kaul S. Microvascular rheology of definity microbubbles following intra-arterial and intravenous administration. J Am Soc Echocardiogr 2002;15:396–403.
4. Lindner JR, Coggins MP, Kaul S, Klibanov AL, Brandenburger GH, Ley K. Microbubble persistence in the microcirculation during ischaemia/reperfusion and inflammation is caused by integrin and complement mediated adherence to activated leukocytes. Circulation 2000;101:668–75.
5. Lindner JR, Song J, Xu F, et al. Noninvasive ultrasound imaging of inflammation using microbubbles targeted to activated leukocytes. Circulation 2000;102:2745–50.
6. Fisher NG, Christiansen JP, Leong-Poi H, Jayaweera AR, Lindner JR, Kaul S. Myocardial and microcirculatory kinetics of BR14, a novel third generation intravenous ultrasound contrast agent. J Am Coll Cardiol 2002;39:530–7.
7. Chonn A, Cullis PR, Devine DV. The role of surface charge in the activation of the classical and alternative pathways of complement by liposomes. J Immunol 1991;146:4234–41.
8. Chonn A, Semple SC, Cullis PR. Association of blood proteins with large unilamellar liposomes in vivo: relation to circulation lifetimes. J Biol Chem 1992;267:18759–65.
9. Devine DV, Wong K, Serrano K, Chonn A, Cullis PR. Liposome-complement interactions in rat serum: implications for liposome survival studies. Biochim Biophys Acta 1994;1191:43–51.
10. Du H, Chandaroy P, Hui SW. Grafted poly-(ethylene glycol) on lipid surfaces inhibits a protein adsorption and cell adhesion. Biochim Biophys Acta 1997;1326:236–48.
11. Efremova NV, Bondurant B, O'Brien DF, Leckband DE. Measurements of interbilayer forces and protein adsorption on uncharged lipid bilayers displaying poly(ethylene glycol) chains. Biochemistry 2000;39:3441–51.
12. Wilson WW, Wade MM, Holman SC, Champlin FR. Status of methods for assessing bacterial cell surface charge properties based on zeta potential measurements. J Microbiol Methods 2001;43:153–64.
13. Thompson MK, Starmer CF, Whorten RE, McIntosh MD. Indicator transit time considered as a gamma variate. Circ Res 1964;14:502–15.
14. Keller MW, Feinstein SB, Watson DD. Successful left ventricular opacification following peripheral venous injection of sonicated contrast agent: an experimental evaluation. Am Heart J 1987;114:570–5.
15. Leszewiski MK, Atkinson JP. Endothelial cell responses to complement activation. In: Volankis JE, Frank MM, editors. The Human Complement System in Health and Disease. New York, NY: Marcel Dekker, 1998:149–67.

16. Saadi S, Platt JL. Endothelial cell responses to complement activation. In: Volankis JE, Frank MM, editors. The Human Complement System in Health and Disease. New York, NY: Marcel Dekker, 1998:335–55.
17. Ciurea D, Gil J. Morphometry of capillaries in three zones of rabbit lungs fixed by vascular perfusion. Anat Rec 1996;244:182–92.
18. Price ME, Cornelius RM, Brash JL. Protein adsorption to polyethylene glycol modified liposomes from fibrinogen solution and from plasma. Biochim Biophys Acta 2001;1512:191–205.
19. Klibanov AL, Maruyama K, Torchilin VP, Huang L. Amphipathic polyethyleneglycols effectively prolong the circulation time of liposomes. FEBS Lett 1990;268:235–7.
20. Klibanov AL, Maruyama K, Beckerleg AM, Torchilin VP, Huang L. Activity of amphipathic poly(ethylene glycol) 5000 to prolong the circulation time of liposomes depends on the liposome size and is unfavorable for immunoliposome binding to target. Biochim Biophysic Acta 1991;1062:142–8.
21. Torchilin VP, Omelyanenko VG, Papisov MI, et al. Poly(ethylene glycol) on the liposome surface: on the mechanism of polymer-coated liposome longevity. Biochim Biophysic Acta 1994;1195:11–20.
22. Grayburn PA, Erickson JM, Escobar J, Womack L, Velasco. Peripheral intravenous myocardial contrast echocardiography using a 2% dodecafluoropentane emulsion: identification of myocardial risk area and infarct size in the canine model of ischemia. J Am Coll Cardiol 1995;26:1340–7.
23. Beppu S, Matsuda H, Shishido T, Matsumura M, Miyatake K. Prolonged myocardial contrast echocardiography via peripheral venous administration of QW3600 injection (Echogen): its efficacy and side effects. J Am Soc Echocardiogr 1997;10:11–24.
24. Sontum PC, Walday P, Dyrstad K, Hoff L, Frigstad S, Chistiansen C. Effect of microsphere size distribution on the ultrasonographic contrast efficacy of air-filled albumin microspheres in the left ventricle of dog hearts. Invest Radiol 1997;32:627–35.